THE MULTI-PHASE GASEOUS HALOS OF LATE-TYPE SPIRALS

R. Tüllmann[1], W. Pietsch[2], J. Rossa[3], D. Breitschwerdt[4], and R.-J. Dettmar[1]

[1]Astronomisches Institut, Ruhr-Universität Bochum, 44780 Bochum, Germany
[2]Max-Planck Institut für extraterrestrische Physik, 85748 Garching, Germany
[3]Space Telescope Science Institute, Baltimore, MD 21218, U.S.A.
[4]Institut für Astronomie, Universität Wien, 1180 Wien, Austria

ABSTRACT

First results from an X-ray mini-survey carried out with XMM-Newton are presented in order to investigate the diffuse Hot Ionized Medium in the halos of nine star-forming edge-on galaxies. Diffuse X-ray halos were detected in eight of our targets, covering a wide range of star formation rates from quiescent to starburst cases. EPIC X-ray contour maps overlaid onto Hα imaging data revealed that the presence of X-ray halos is correlated with Diffuse Ionized Gas. Moreover, these halos are associated with non-thermal cosmic ray halos, as evidenced by radio continuum observations. UV-data obtained with the OM-telescope reveal that Diffuse Ionized Gas is well associated with UV emission originating in the disk. We found very strong indications that spatially correlated multi-phase gaseous halos are associated with star forming processes in the disk. By including multi-wavelength data of other star forming spirals, we obtained a sample of 23 galaxies which allow us to test key parameters which trigger the formation of multi-phase halos. We found that diffuse soft (0.3-2.0 keV) X-ray luminosities correlate well with Hα, B-band, FIR, UV, and radio continuum luminosities, with SFRs and with the energy input rate by SNe. X-ray luminosities are found to not correlate with HI mass and baryonic mass. All this implies that gaseous halos are indeed created by star forming processes. Moreover, there seems to exist a critical SFR threshold above which these halos form.

Key words: Galaxy halos; extended X-ray emission; ISM; starburst and quiescent galaxies.

1. INTRODUCTION

What causes the formation of multi-phase gaseous halos in star forming late-type spiral galaxies? It is commonly believed that supernova (SN) explosions, galactic winds or stellar winds from young and hot stars are the main triggering mechanisms. Theoretical models predict an intense transport of gas and momentum between the disk plane and the halo (so called disk-halo interaction, DHI). The combined power of SNe explosions in star forming regions produce overpressured flows of hot gas which is driven off the disk into the halo. This process gives rise to phenomena known as galactic fountains (de Avillez, 2000) or chimneys (Norman & Ikeuchi, 1989).

The results of the violent energy input are visible in different wavelength regions, such as in the radio, in the optical or in X-rays. Superbubbles and filaments as well as extended worm structures have been observed in the Milky Way (e.g., Heiles, 1984; Koo et al., 1992; Reynolds et al., 2001) as well as in several other galaxies (e.g., Devine & Bally, 1999; Tüllmann et al., 2000, 2003).

Independent evidence of an interstellar DHI comes from the presence of a thick extraplanar layer (1.5 – 10 kpc) of ionized hydrogen, called "Diffuse Ionized Gas" (DIG) which is most likely also blown out into the halo by correlated SNe (see Dettmar (2004) for a recent review). During the last five years significant progress was achieved in this field, e.g., by carrying out a comprehensive Hα survey of 74 edge-on spirals, by estimating the ejected DIG mass, and deriving an empirical set of parameters which indicates the presence of prominent DIG halos (Rossa & Dettmar, 2000, 2003a,b). It turned out that the star formation rate (SFR) per unit area determines whether or not starburst and normal star forming galaxies possess DIG halos. As the SFR is related to the energy input rate by SNe, this directly supports star formation induced galaxy halos.

Moreover, it was shown that filamentary DIG structures (traced by Hα), radio continuum emission, and magnetic field vectors are well aligned in the halos of some star forming spirals (e.g., Dahlem et al., 1997; Tüllmann et al., 2000). This was verified also for at least 13 of the survey galaxies for which radio data are available (Rossa & Dettmar, 2003a,b). Beside this purely morphological correlation, additional studies also found correlations between FIR, B, and X-ray luminosities (e.g., Condon,

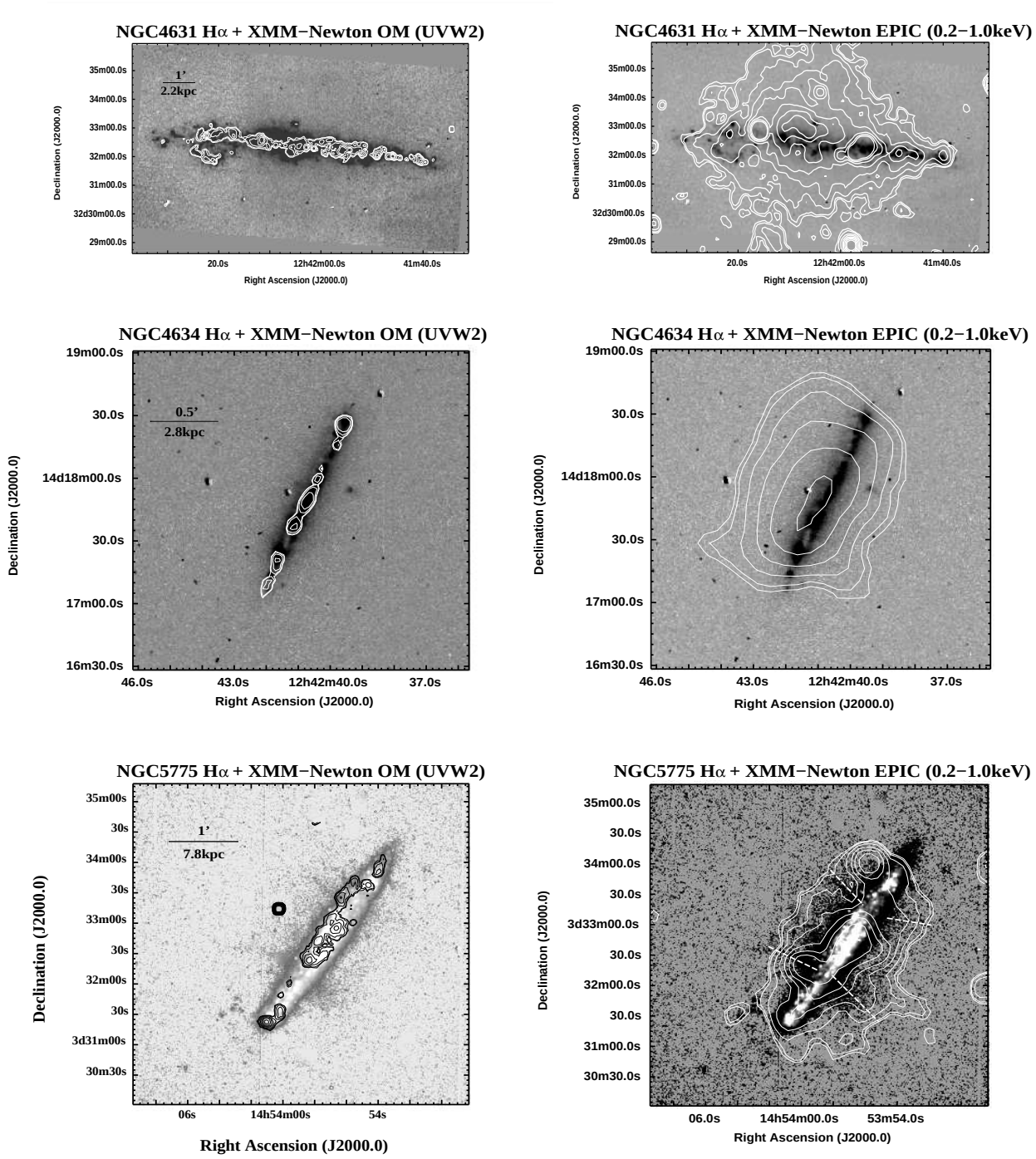

Figure 1. The UV contours maps of NGC 4631, NGC 4634, and NGC 5775 (left panels) obtained with the Optical Monitor (UVW2 filter) and overlaid onto corresponding Hα images nicely confirm the tight relation between DIG and UV continuum emission. The appropriate EPIC X-ray images (right panels) were created from merged pn and MOS eventlists in the soft energy-band (0.2 - 1.0 keV) and give evidence to the presence of soft extended X-ray halos.

1992; Read & Ponman, 2001). For starburst galaxies, a multi-phase correlation could be established making extensive use of the Chandra satellite (Strickland et al., 2002, 2004a,b) and XMM-Newton (Stevens et al., 2003; Ehle, 2005). For normal star forming spirals, however, it was dubious, until we started to investigate the above relation with XMM-Newton for lower energy input rates.

What causes the coexistence of multi-phase gaseous halos? This can be understood by considering the origin of the radiation observed in certain wave bands. The FIR emission is most likely produced by young dust enshrouded stars whose UV flux is absorbed by dust grains and re-emitted at infrared wavelengths. Synchrotron emission originates in the radio continuum and traces

Table 1. Derived plasma parameters

Galaxy	D	$\|z\|$	$kT_{\rm soft}$	$kT_{\rm hard}$	$L_{\rm X,soft}$	$n_{\rm e,soft}$	$n_{\rm e,hard}$	$<M_{\rm gas}>$
	[Mpc]	[kpc]	[keV]		[10^{40} erg s^{-1}]	$\times10^{-3}/\sqrt{f}$ [cm^{-3}]		$\times10^{8} f$ [M$_\odot$]
	(1)	(2)	(3)	(4)	(5)	(6)	(7)	(8)
		10.6	0.062 ± 0.037	0.196 ± 0.074	0.02	0.5±0.2	0.6±0.3	0.01±≤0.01
		9.00	0.069 ± 0.032	0.245 ± 0.041	0.03	0.7±0.2	0.8±0.3	0.01±≤0.01
		7.40	0.096 ± 0.038	0.211 ± 0.075	0.07	0.9±0.1	1.1±0.2	0.07±0.02
		5.80	0.103 ± 0.019	0.274 ± 0.035	0.12	1.3±0.2	1.5±0.3	0.10±0.03
		4.20	0.173 ± 0.031	0.284 ± 0.057	0.15	1.5±0.2	1.8±0.3	0.11±0.04
NGC 4631	7.5	0.0	0.234 ± 0.012	0.867 ± 0.019	0.25	0.7±0.1	0.9±0.2	0.44±0.10
		2.90	0.173 ± 0.029	0.372 ± 0.093	0.08	1.0±0.1	1.2±0.2	0.09±0.03
		4.50	0.151 ± 0.037	0.266 ± 0.124	0.04	0.8±0.1	0.9±0.2	0.06±0.02
		6.10	0.122 ± 0.028	0.271 ± 0.181	0.02	0.6±0.1	0.7±0.1	0.03±0.01
		3.30	0.093 ± 0.012	0.191 ± 0.089	0.03	1.3±0.2	1.5±0.4	0.02±≤0.01
		1.90	0.108 ± 0.032	0.267 ± 0.113	0.05	1.8±0.3	2.0±0.6	0.03±0.01
NGC 4634	19.1	0.0	0.227 ± 0.035	0.848 ± 0.207	0.03	1.3±0.2	1.8±0.3	0.03±≤0.01
		2.00	0.113 ± 0.027	0.305 ± 0.130	0.04	1.4±0.2	1.6±0.5	0.03±0.02
		6.90	0.067 ± 0.031	0.251 ± 0.101	0.16	0.6±0.2	0.7±0.3	0.28±0.19
		4.20	0.085 ± 0.022	0.280 ± 0.053	0.36	0.9±0.2	1.0±0.3	0.41±0.22
NGC 5775	26.7	0.0	0.263 ± 0.049	0.940 ± 0.191	0.37	2.6±0.1	3.6±0.2	1.65±0.22
		4.40	0.125 ± 0.033	0.358 ± 0.136	0.42	1.0±0.2	1.1±0.3	0.45±0.18
		7.05	0.099 ± 0.029	0.350 ± 0.168	0.24	0.7±0.2	0.8±0.3	0.34±0.20

Notes: Col (1): Distance to the target in Mpc. Col. (2): Height above/below the disk plane where the spectrum was extracted. Cols. (3) and (4): Temperatures for the soft and hard component as derived from spectral fitting (see Tüllmann et al. 2005 for details). Col. (5): Diffuse soft X-ray luminosities (0.3 – 2.0 keV), based on distances listed in Col. (1). Cols. (6) to (7): Electron densities for the soft and hard component. Col. (8): Averaged gas masses within the extracted volume, based on averaged electron densities calculated from Cols. (6) and (7).

high energy cosmic ray (CR) electrons produced by SNe or Supernova remnants (SNRs). B-band and UV luminosities are indicators of the continuum radiation of hot and young stars, whereas Hα is a good tracer of gas photoionized by OB-stars and of the above mentioned DHI. X-ray emission, finally, is typical for X-ray binaries, SNRs, superwinds, and diffuse hot plasmas generated by these objects.

2. THE SAMPLE

Our initial XMM-Newton sample consists of nine star forming late-type spiral galaxies which cover the starburst as well as the quiescent case. All targets are nearby to gain good spatial resolution and seen nearly edge-on to allow a clear discrimination between the soft emission originating in the disk and the halo. The sample was chosen from the aforementioned Hα survey of edge-on galaxies (Rossa & Dettmar, 2003a) by selecting galaxies with the highest $L_{\rm FIR}/D_{25}^2$ values and exceeding a IRAS S_{60}/S_{100} ratio of 0.3. These parameters are considered to be a good discriminator for starburst and normal star forming spiral galaxies (e.g., Lehnert & Heckman, 1996; Rossa & Dettmar, 2003a; Strickland et al., 2004a). It should be stressed that our sample is neither complete nor free from selection effects.

3. RESULTS

In the following we concentrate on presenting representative results for two starburst galaxies (NGC 4631 and NGC 5775) and one actively star forming spiral galaxy (NGC 4634). We used merged EPIC pn and MOS contour maps (0.2 –1.0 keV) overlaid onto Hα images and of Optical Monitor (OM) UV imagery carried out with the UVW2 filter in order to systematically investigate the spatial correlation of multi-phase gaseous galaxy halos. A detailed description of our multi wavelength approach and relevant results from our XMM-Newton observations are given in the first of a series of papers (Tüllmann et al., 2005).

3.1. XMM-Newton EPIC and OM imaging

Fig. 1 nicely confirms that the extraplanar DIG emission is well associated with sites where the UV-flux in the disk is enhanced. In case of NGC 5775, one likely can interpret the extraplanar DIG as the limb brightened walls of giant outflow cones and thus make the connection with the central UV sources which seem to be the main drivers of the outflow. Hence, in all three cases a clear correlation between DIG and UV continuum originating in the disk plane exists. As DIG also correlates with diffuse soft X-ray emitting gas in the halo (see right-hand panels), it

is self-evident to also consider a correlation between the hot ionized gas and stellar feedback processes (traced by UV radiation).

Beside a DIG and a soft X-ray halo, all three targets also show an extended radio continuum halo at 1.4 GHz, indicating the presence of CRs at extraplanar distances. Hence, we conclude that multi-phase gaseous halos are indeed created by star forming activity rather than by accretion from the IGM/halo as suggested by Benson et al. (2000) or Toft et al. (2002).

What, however, is the critical energy threshold above which multi-phase halos start to form? We address this question in subsection 3.3.

3.2. XMM-Newton EPIC pn spectroscopy

Essential parameters of the halo gas, such as electron densities, gas temperatures, and gas masses, were determined by means of EPIC pn spectroscopy carried out at several offset positions above the disk (see Table 1). In order to determine these quantities we fitted all spectra with a simple 3-component model, consisting of a photoelectric absorber to account for the foreground absorption and two thermal Raymond-Smith (RS) plasma models. Both RS components (a hard and a soft one) are fixed to cosmic metal abundances. The individual $N_{\rm H}$ values have been taken from Dickey & Lockman (1990) and are not allowed to vary during the χ^2-minimization process.

Spectra are fitted only for energy channels with a significant number of counts per time and energy interval. For the halo this is the range between 0.3 –2 keV, which nicely demonstrates that diffuse X-ray halos are indeed very soft. From Fig. 2 it is directly evident that there is a temperature and density gradient in the halo. Gas temperatures and electron densities decrease with increasing height above the disk. As a consequence of declining densities, the hot ionized gas mass in every extracted region decreases, too. The trends shown in Fig. 2 are consistent with starburst-driven Galactic wind models (Breitschwerdt, 2003).

3.3. Multi-frequency correlations

Provided our hypothesis of star formation induced multi-phase galaxy halos is correct, there also should exist (in addition to phenomenological analogies) strong correlations between different star formation tracers. Such tracers could be star formation rates (SFRs), SN energy input rates ($\dot{E}_{\rm A}^{\rm tot}$) and $L_{\rm FIR}/D_{25}^2$ ratios, but also multi-frequency luminosities of the integrated radio continuum, FIR, Hα, B-band, UV, and X-ray emission.

In order to carry out a statistical correlation analysis of these quantities, we increased our initial sample by

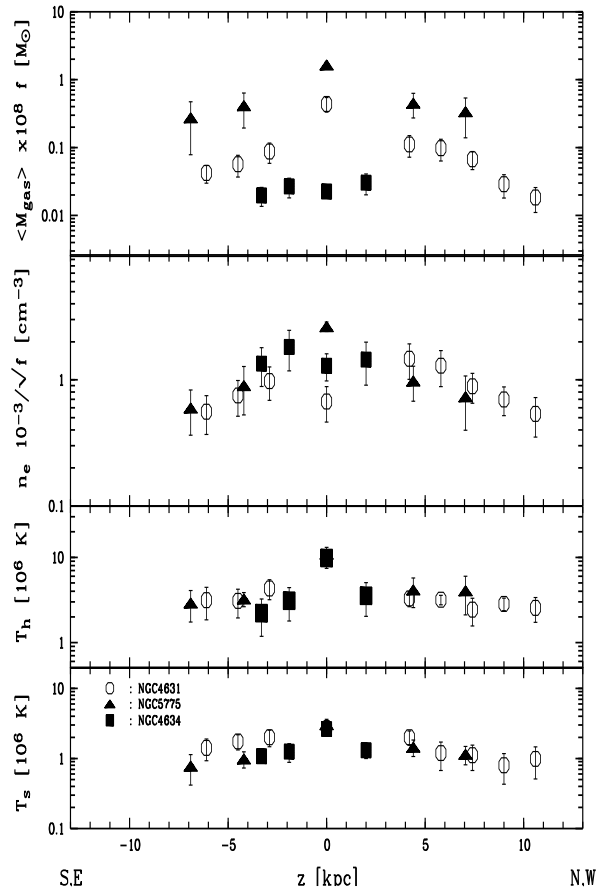

Figure 2. Derived gas parameters plotted as a function of z. Soft and hard temperatures have been derived by fitting the emission spectra with a photoelectric absorber and two RS plasma models of different temperatures. Electron densities and gas masses within the ionized volume are averages of the soft and the hard component and are calculated from soft X-ray luminosities.

searching the literature for appropriate targets. The following sample selection criteria were applied: all galaxies had to be late-type spirals (Sc-Sd), relatively nearby (< 50 Mpc), and seen nearly edge-on ($i > 70°$). Moreover, they had to be previously investigated in the wave bands listed above. No constraints were imposed on the $S60/S100$ and $L_{\rm FIR}/D_{25}^2$ ratios to reach the largest possible coverage of the parameter space. Our extended sample consists now of 23 galaxies which allow us to perform least-squares fitting (assuming $Y = mX + b$) and Spearman rank-order correlation analysis, to test the significance of the correlation between the investigated pairs of parameters. Results are shown in Fig. 3.

We find very strong linear correlations between star formation indicators and multi-frequency luminosities. In addition to the well established $L_{\rm FIR}/L_{1.4\rm GHz}$ relation, highly significant linear dependencies between soft X-ray luminosities (0.3 – 2.0 keV) and integrated FIR, radio continuum (1.4 GHz), Hα, B-band, and UV luminosities can be established. Moreover, soft X-ray lumi-

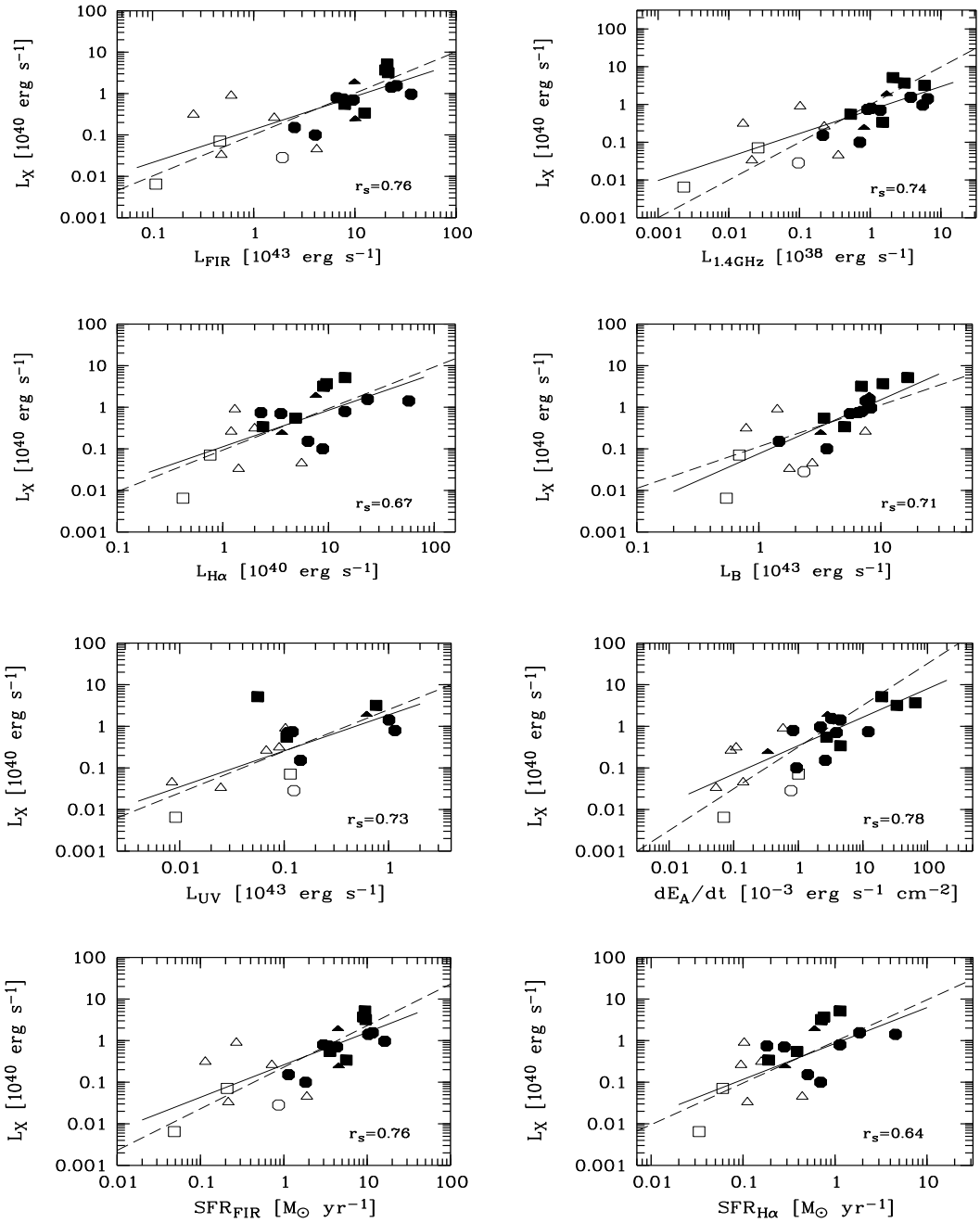

Figure 3. The strong linear correlations between X-ray luminosities, FIR, 1.4 GHz, Hα, broadband B, and UV luminosities, SFRs, and energy input rates $\dot{E}_{\rm A}$, indicate that star forming processes in the disk are the likely driver of multi-phase gaseous halos. Filled (open) symbols represent galaxies with(out) multi-phase halo detections. Solid lines represent the best linear fits to the data whereas the dashed line indicates a relation with unity slope (see Tüllmann et al. (2005b) for details and the full set of correlations). r_s denotes the Spearman rank-order correlation coefficient.

nosities correlate well with star formation rates and the energy input rate by SNe into the ISM. Only weak correlations are found between the dust mass of a galaxy and the corresponding soft X-ray luminosity. X-ray luminosities are found to not correlate with baryonic and H I gas masses. These statistical results also support that multi-phase gaseous galaxy halos in late-type spiral galaxies are created by outflowing gas produced in star forming related events in the disk plane.

However, in order to achieve a more comprehensive picture on the evolution of galaxy halos in different wave bands, we need to answer the question of the threshold SFR (or equivalently the SN energy input rate $\dot{E}_A$) re-

quired to create multi-phase gaseous halos. From Fig. 3 we cannot tell precisely, as the lower energy end of our correlations is statistically not well covered. It appears, however, that for multi-phase halos to evolve a critical threshold needs to be exceeded (e.g., a $SFR_{\rm FIR} \geq 1.0\,{\rm M}_\odot$/yr). Interestingly, DIG seems to coexist with other gas components if a Hα star formation rate per unit area of $(3.2 \pm 0.5) \times 10^{40}$ erg s^{-1} kpc^{-2} is exceeded (Rossa & Dettmar, 2003b).

In this context it is important to point out that the quantification of the threshold and the progress of understanding the physics of gaseous galaxy halos now depends on galaxies with no or only little halo emission than on "well understood" targets.

4. SUMMARY AND CONCLUSIONS

With a sample of 23 normal star forming galaxies and by adding additional wave bands (Hα and UV), we found remarkably strong linear correlations between 1.4GHz radio continuum, FIR, Hα, B-band, UV, and X-ray luminosities. Strong correlations also exist if X-ray luminosities are plotted against SFRs, $L_{\rm FIR}/D_{25}^2$, or the energy input rate by SNe per unit area, expressed by $\dot{E}_{\rm A}$ (cf. Fig. 3). X-ray luminosities neither correlate with the H I nor with the baryonic mass of a galaxy. Our results clearly imply that multi-phase halos are the consequence of stellar feedback processes in the disk plane. They conflict with the concept of halos being due to infalling gas from the IGM.

REFERENCES

Benson, A. J., Bower, R. G., Frenk, C. S., & White, S. D. M. 2000, MNRAS, 314, 557

Breitschwerdt, D. 2003, RevMexAA, 15, 311

Condon, J. J. 1992, ARA&A, 30, 575

Dahlem, M., Petr, M., Lehnert, M. D., Heckman, T. M., & Ehle, M. 1997, A&A, 320, 731

de Avillez, M. A., 2000, MNRAS, 315, 479

Dettmar, R.–J. 2004, Ap&SS, 289, 349

Devine, D., & Bally, J. 1999, ApJ, 510 197

Dickey, J. M., & Lockman, F. J. 1990, ARA&A, 28, 215

Ehle, M. 2005, in: "Extra-planar Gas", ed. R. Braun, ASP Conf. Series, 331, 337

Heiles, C. 1984, ApJS, 55, 585

Koo, B.-C., Heiles, C., & Reach, W. T. 1992, ApJ, 390, 108

Lehnert, M. D., & Heckman, T. M. 1996, ApJ, 472, 546

Norman, C. A., & Ikeuchi, S. 1989, ApJ, 345, 372

Read, A. M., & Ponman, T. J. 2001, MNRAS 328, 127

Reynolds, R. J., Sterling, N. C., & Haffner, L. M. 2001, ApJ, 558, L101

Rossa, J., & Dettmar, R.–J. 2000, A&A, 359, 433

Rossa, J., & Dettmar, R.–J. 2003a, A&A, 406, 493

Rossa, J., & Dettmar, R.–J. 2003b, A&A, 406, 505

Stevens, I. R., Read, A. M., & Bravo-Guerrero, J. 2003, MNRAS, 343, L47

Strickland, D. K., Heckman, T. M., Weaver, K. A., Hoopes, C. G., & Dahlem, M. 2002, ApJ, 568, 689

Strickland, D. K., Heckman, T. M., Colbert, E. J. M., Hoopes, C. G., & Weaver, K. A. 2004a, ApJS, 151, 193

Strickland, D. K., Heckman, T. M., Colbert, E. J. M., Hoopes, C. G., & Weaver, K. A. 2004b, ApJ, 606, 829

Toft, S., Rasmussen, J., Sommer-Larsen, J., & Pedersen, K. 2002, MNRAS, 335, 799

Tüllmann, R., Dettmar, R.–J., Soida, M., Urbanik, M., & Rossa, J. 2000, A&A, 364, L36

Tüllmann, R., Rosa, M. R., Elwert, T., Bomans, D. J., Ferguson, A. M. N., & Dettmar, R.–J. 2003, A&A, 412, 69

Tüllmann, R., Pietsch, W., Rossa, J., Breitschwerdt, D., & Dettmar, R.-J. 2005a, accepted for publication in A&A, astro-ph/0510079

Tüllmann, R., Pietsch, W., Rossa, J., Breitschwerdt, D., & Dettmar, R.-J. 2005b, in prep.